Boundary streaming by internal waves

Antoine Venaille, Antoine Renaud

Boundary streaming by internal waves

A. Renaud†, A. Venaille‡

Univ Lyon, Ens de Lyon, Univ Claude Bernard, CNRS, Laboratoire de Physique, F-69342 Lyon, France

(Received xx; revised xx; accepted xx)

Damped internal wave beams in stratified fluids have long been known to generate strong mean-flows through a mechanism analogous to acoustic streaming. While the role of viscous boundary layers in acoustic streaming has thoroughly been addressed, this remains largely unexplored in the case of internal waves. Here we compute the mean-flow generated close to an undulating wall that emits internal waves in a viscous, linearly stratified two-dimensional Boussinesq fluid. Using a quasi-linear approach, we show that the mean-flow behavior depends strongly on the boundary conditions, and find good agreement with numerical simulations. We apply these computations to an idealised model for the quasi-biennial oscillation, and find that the presence of boundary layers have a qualitative impact on the period of flow reversals within the domain bulk.

Key words:

1. Introduction

Internal gravity waves play a crucial role in the dynamics of atmospheres and oceans as they redistribute energy and momentum (Sutherland 2010). In particular, strong mean-flows can be generated by non-linear effects within internal wave beams (Lighthill 1978), a phenomenon analogous to acoustic streaming (Riley 2001). A striking example of internal wave streaming is the quasi-biennial oscillation of equatorial zonal winds in the stratosphere driven by damped internal gravity waves (Baldwin *et al.* 2001). This is a robust phenomenon that has also been reproduced in a celebrated laboratory experiment (Plumb & McEwan 1978). In that case, the classical explanation of streaming relies on the damping of the wave within the domain bulk. Other instances of bulk streaming have then been reported in numerical simulations (Grisouard & Bühler 2012), laboratory experiments (King *et al.* 2009; Bordes *et al.* 2012; Semin *et al.* 2016), and a self-consistent theory for the generation of vortical mean-flows in the domain bulk has been proposed (Kataoka & Akylas 2015). None of these studies have addressed the role of viscous boundary layers and their potential implications for the generation of mean-flows confined to the boundary, by contrast with acoustic waves, that have long been known to produce strong mean-flow within their viscous boundary layers (Zarembo 1971; Xie & Vanneste 2014). This is surprising, given that boundaries are central to the generation of the waves in laboratory experiments (Gostiaux *et al.* 2006) and numerical models (Legg 2014), or to their effect on energy focusing through multiple reflections (Maas *et al.* 1997). Viscous internal wave beams generated by boundaries have been extensively studied (Voisin 2003), together with their consequences on the energy budget of numerical ocean

† Email address for correspondence: antoine.renaud@ens-lyon.fr
‡ Email address for correspondence: antoine.venaille@ens-lyon.fr

models (Shakespeare & Hogg 2017). Importance of viscous boundary layers for the energy budget of internal wave attractors have recently been addressed (Beckebanze & Maas 2016). However, mean-flow generation associated with viscous boundary layers have not been discussed. Here we compute in a two-dimensional, quasi-linear framework the mean-flow generated by internal gravity waves close to a boundary, paying particular attention to the role of boundary conditions. The importance of changing boundary condition in numerical models of internal wave dynamics close to bottom topography has been noticed in previous work related to mixing and wave dissipation (Nikurashin & Ferrari 2010). We will show that changing boundary conditions also substantially affects wave-driven mean-flows. The quasi-linear approach is introduced in section 2. The structure of the viscous linear waves and their induced Reynolds stresses are presented in section 3. The consequences for mean-flow generation are discussed in 4, together with an application to an idealised model of the quasi-biennial oscillation. A WKB treatment of the problem is provided in appendix A.

2. Zonally symmetric waves and mean-flow interaction

We consider a fluid within a two-dimensional domain, periodic in the zonal x-direction with period L and semi-infinite in the vertical z-direction. We leave for future work the study of three-dimensional effects, that are known to be central to streaming effects in the domain bulk (Grisouard & Bühler 2012; Bordes *et al.* 2012; Kataoka & Akylas 2015).The bottom boundary is a vertically undulating line located on average at $z = 0$, whose equation is given by $z = h(x, t)$. We consider an incompressible viscous Boussinesq fluid with viscosity ν and linearly stratified with buoyancy frequency N. For the sake of simplicity, we do not consider any diffusion process for the buoyancy. This hypothesis is relevant for experimental configurations when the stratification agent is salt given the low diffusivity $\kappa = \nu/1000$. We also consider a linear friction term for the velocity field with coefficient γ, thought to be a crude model for possible lateral boundaries (Plumb & McEwan 1978; Semin *et al.* 2016).

The dynamical equations writes:

$$\begin{cases} \partial_t \mathbf{u} + (\mathbf{u}\cdot\nabla)\,\mathbf{u} & = -\nabla p + b\mathbf{e}_z - \gamma\mathbf{u} + \nu\nabla^2\mathbf{u} \\ \partial_t b + \mathbf{u}\cdot\nabla b + N^2 w & = 0 \\ \nabla\cdot\mathbf{u} & = 0 \end{cases} \tag{2.1}$$

where $\mathbf{u} = (u, w)$ is the two-dimensional velocity, p the renormalised pressure, b the buoyancy anomaly and $\nabla^2 = \partial_{xx} + \partial_{zz}$ the standard Laplacian operator.

In this paper, we discuss two different bottom boundary conditions on $z = h(x, t)$:

$$\text{free-slip:}\quad w = \partial_t h\ ,\ \boldsymbol{S}[\mathbf{n}_h]\cdot\mathbf{n}_h^{\perp} = 0 \quad ; \quad \text{no-slip:}\quad \mathbf{u} = \partial_t h\mathbf{e}_z \tag{2.2}$$

where $\mathbf{n}_h = \nabla(z - h(x, t))$ is a local normal vector of the bottom boundary, $\mathbf{n}_h^{\perp}$ a local tangent vector and $\boldsymbol{S}$ the shear stress tensor ($S_{ij} = \partial_j u_i$).

The free-slip boundary condition is considered in many oceans numerical models when the viscous shear layer is not resolved (see e.g. Legg 2014). When considering a progressive pattern ($h(x, t) = h(x - ct)$) in 2.2, a Galilean change of referential brings us to the case of the lee-waves generation by barotropic mean-flow passing over a bottom topography. All the predictions concerning the free-slip boundary condition will be compared against direct numerical simulations of monochromatic lee-waves generation using the MIT global circulation model (Adcroft *et al.* 1997) which specifically uses our definition for the free-slip condition. The no-slip boundary condition in (2.2) is relevant to model the generation

of internal gravity waves in laboratory experiments using vertically oscillating bottom boundaries such as in Plumb & McEwan (1978) or Semin *et al.* (2016).

They are four independent dimensionless numbers in the problem. Let us consider k and ω, the typical zonal wave number and angular frequency for the bottom oscillations. The Froude number $Fr = \omega/N$ controls the propagation of the inviscid wave. We define a Reynolds number based on the wave properties, $Re = \omega/\left(k^2\nu\right)$, controlling the viscous damping and the viscous boundary layers thickness. When considering the lee-wave generation case, this Reynolds number can be linked to the standard Reynolds number $Re = UL/\nu$ where U is the typical mean zonal velocity. An amplitude parameter for the wave is given by the typical slope of the bottom boundary, $\epsilon = h_b k$, where h_b is the typical amplitude of h. In this paper, the considered amplitude parameters are small enough to neglect triadic interactions of waves. Finally, the rescaled friction coefficient $\tilde{\gamma} = \gamma/\omega$ controls the frictional damping of the wave. An additional aspect ratio number $R = kH$ has to be taken into account in numerical simulation where the domain has a finite height H.

We decompose any field ϕ into a mean-flow $\overline{\phi}$ and a wave ϕ' using the zonal averaging procedure (see Bühler 2009):

$$\overline{\phi}\,(z,t) = \frac{1}{L}\int_0^L \mathrm{d}x\;\phi\,(x,z,t)\,, \quad \phi' = \phi - \overline{\phi}. \tag{2.3}$$

The averaging of the zonal momentum equation in (2.1) leads to the mean zonal-momentum equation:

$$\partial_t \overline{u} = -\partial_z \overline{u'w'} - \gamma\overline{u} + \nu\partial_{zz}\overline{u}. \tag{2.4}$$

By subtracting the averaged equations from (2.1) and linearizing the result, we obtain the wave equations

$$\begin{cases} \partial_t u' + \overline{u}\partial_x u' + w'\partial_z\overline{u} & = -\partial_x p' - \gamma u' + \nu\nabla^2 u' \\ \partial_t w' + \overline{u}\partial_x w' & = -\partial_z p' + b' - \gamma w' + \nu\nabla^2 w' \\ \partial_t b' + \overline{u}\partial_x b' + N^2 w' & = 0 \\ \partial_x u' + \partial_z w' & = 0 \end{cases} \tag{2.5}$$

Wave-wave interactions are ignored in the present model. The coupled equations (2.4) and (2.5) form a quasi-linear model for the interaction between boundary generated viscous waves and the zonal mean-flow. The Reynolds stress, $\partial_z\overline{u'w'}$, at the origin of streaming, is the only non-linearity kept. It acts as a forcing term and is computed from the wave field. We further assume that the time scale given by the damping length scale divided by the inviscid vertical group velocity of the wave is much smaller than the time scale of the evolution for the mean-flow. Hereby, we assume that the wave field is always the steady response of the boundary within a frozen mean-flow medium. This assumption breaks in the presence of critical layers (see Bühler 2009).

We perform the wave-mean decomposition on the boundary conditions (2.2) and, assuming a small amplitude bottom oscillation ($\epsilon \ll 1$), we linearize the result on a asymptotically flat boundary at $z = 0$:

$$\text{free-slip:} \quad \begin{cases} \partial_z\overline{u} & = 0 \\ w' - \partial_t h & = 0 \\ \partial_z u' & = 0 \end{cases} \quad ; \quad \text{No-slip:} \quad \begin{cases} \overline{u} & = 0 \\ w' - \partial_t h & = 0 \\ u' - h\partial_z\overline{u} & = 0 \end{cases}, \tag{2.6}$$

In the free-slip case, the Reynolds stress vanishes at the bottom ($\partial_z\overline{u'w'}|_{z=0} = 0$), while, in the no-slip case there is no momentum injected in the wave ($\overline{u'w'}|_{z=0} = 0$).

Given that $\overline{u'w'}|_{z=+\infty} = 0$ for damped waves, the integrated streaming has to be zero, $\int_0^\infty \partial_z \overline{u'w'}\,\mathrm{d}z = 0$. All the streaming far from the bottom boundary has to be compensated by an opposite boundary streaming. In the next section, we look at the Reynolds stresses for both boundary conditions at the early stage of the mean-flow evolution when the mean-flow is still weak.

3. Boundary generated viscous waves

In this section, we are interested in the wave equations (2.5) with $\overline{u} = 0$. Let us look for plane wave solutions, $(u', w', b', p') = \Re\left[\left(\tilde{u}, \tilde{w}, \tilde{b}, \tilde{p}\right) e^{i(kx+mz-\omega t)}\right]$, where $\omega > 0$ and $k > 0$ will be fixed by the bottom boundary conditions. By injecting this ansatz in (2.5), we get the dispersion relation for the viscous internal gravity waves:

$$\omega^2 \left(1 + i\frac{\nu\left(k^2+m^2\right)+\gamma}{\omega}\right) = N^2 \frac{k^2}{k^2+m^2}. \tag{3.1}$$

The inviscid dispersion relation, recovered by setting $(\nu, \gamma) = 0$, has two real solutions, $m_0 = k\sqrt{Fr^{-2}-1}$ and its opposite, corresponding to upwardly or downwardly propagating waves. From now on and until further notice we consider $\gamma = 0$. For viscous waves, we retain the upwardly propagating ones by discarding the solutions of (3.1) with a negative imaginary part. The general expressions of the two remaining solutions can be written explicitly but we rather consider the asymptotic expressions for $\nu \ll 1$ which simplifies the discussion:

$$\left\{\begin{array}{ll} m_w & = -m_0 + i/2L_\nu + o\left(\nu\right) \\ m_{bl} & = \left(1+i\right)/\delta_\nu + o\left(\sqrt{\nu}\right) \end{array}\right. \tag{3.2}$$

with

$$\left\{\begin{array}{ll} L_\nu & = k^{-1} ReFr^3\sqrt{1-Fr^2} \\ \delta_\nu & = k^{-1}\sqrt{2/Re} \end{array}\right. \tag{3.3}$$

The solution m_w corresponds to the propagating solution converging toward the inviscid solution in the limit $\nu \to 0$. L_ν is the damping length-scale of the viscous wave scaling with the inverse of the viscosity. The solution m_{bl} corresponds to the boundary layer solution diverging in the limit $\nu \to 0$. The boundary layer thickness given by δ_ν scales like the square root of the viscosity as in the classical case of an oscillating flat boundary. This last solution is needed to match the propagating solution with the viscous boundary conditions. Shakespeare & Hogg (2017) considered the effect of viscous (and diffusive) damping on the propagative solution, but ignored the boundary layer terms.

In the case of a progressive sine-shaped bottom undulations, $h\left(x,t\right) = h_b \Re\left[e^{i(kx-\omega t)}\right]$, the general expression of the wave field is given by linear combination of a propagating and a boundary layer part:

$$\left[u', w', b', p'\right] = \Re\left\{\phi_w \mathbf{P}[m_w]\, e^{i(kx+m_w z-\omega t)} + \phi_{bl}\mathbf{P}\left[m_{bl}\right] e^{i(kx+m_{bl}z-\omega t)}\right\}. \tag{3.4}$$

where $\mathbf{P}[m] = \left[\omega/k, -\omega/m, iN^2/m, N^2/\left(k^2+m^2\right)\right]$ is the polarization of the plane wave obtained from (2.5) and (ϕ_w, ϕ_{bl}) are dimensionless amplitude factors determined by the boundary conditions (2.6):

$$\text{free-slip:} \quad \left\{\begin{array}{ll} \phi_w & = ih_b \frac{m_w m_{bl}^2}{m_w^2 - m_{bl}^2} \\ \phi_{bl} & = ih_b \frac{m_{bl} m_w^2}{m_{bl}^2 - m_w^2} \end{array}\right. ; \quad \text{No-slip:} \quad \left\{\begin{array}{ll} \phi_w & = ih_b \frac{m_w m_{bl}}{m_w - m_{bl}} \\ \phi_{bl} & = ih_b \frac{m_w m_{bl}}{m_{bl} - m_w} \end{array}\right. . \tag{3.5}$$

Let us remark that, on top of the inviscid linearity criterion $m_0 h_b \ll 1$, there is an

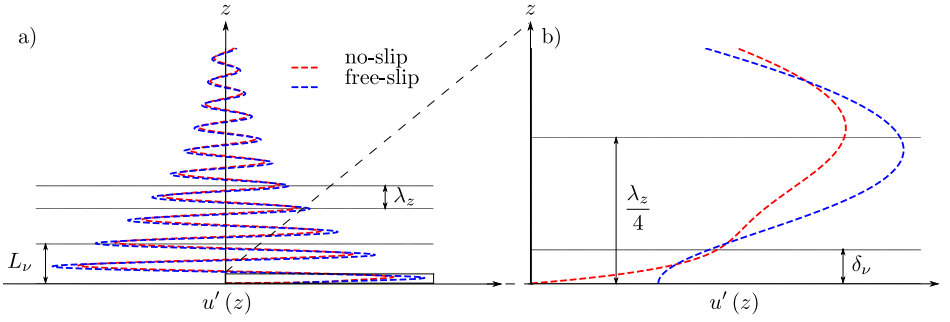

FIGURE 1. a)Example of a linear computation of the vertical profile of the fully established wave field, u', in the absence of mean-flow with the free-slip (orange) and no-slip (red) boundary conditions. b) Zoom on the boundary layer of the wave. The wave damping length, L_ν, and the boundary layer thickness, δ_ν, are represented on the graph along with the inviscid vertical wave length, $\lambda_z = 2\pi/m_0$.

additional stronger criterion $h_b/\delta_\nu \ll 1$ ensuring the linearity of the boundary layer term. While the wave beam is linear, the boundary layer of the wave can be nonlinear and requires higher harmonics contributions to be well described in that case. To simplify the discussion, we consider the contribution of the mode-1 only.

The generic vertical profiles of the wave field u' are drawn in figure 1 for both boundary conditions. Most of the disagreement between the two profiles is in the boundary layer close to the bottom boundary leading to very different boundary streaming behaviour as we will see by computing the Reynolds stresses.

The total vertical momentum flux, $\overline{u'w'}$, is composed of cross terms involving both the propagative and the boundary layer contributions. In the limit of small viscosity, the "self-interaction" of the propagating contribution decreases exponentially over a scale L_ν. This term induces the bulk streaming. All the other terms involve a pairing with the boundary layer contribution decreasing exponentially over a scale δ_ν. The sum of these terms induces the boundary streaming, which has to our knowledge never been discussed in previous studies of internal waves in stratified fluids. We thus decompose the Reynolds stress into a bulk and a boundary term

$$\partial_z \overline{u'w'}\,(z) = f_w\,(z) + f_{\rm bl}\,(z)\,. \tag{3.6}$$

Without mean-flow, in the small ν limit and for both boundary conditions in (2.6), the two contributions of the Reynolds stress write

$$\text{free-slip:} \quad \begin{cases} f_w\,(z) &= -\frac{kc^2\epsilon^2}{2Fr^4Re} e^{-z/L_\nu} + o\,(\nu) \\ f_{bl}\,(z) &= -\frac{kc^2\epsilon^2}{2Fr^2} e^{-z/\delta_\nu} \sin\frac{z}{\delta_\nu} + o\,(1) \end{cases}$$

$$\text{No-slip:} \quad \begin{cases} f_w\,(z) &= -\frac{kc^2\epsilon^2}{2Fr^4Re} e^{-z/L_\nu} + o\,(\nu) \\ f_{bl}\,(z) &= \frac{kc^2\epsilon^2}{2Fr} \sqrt{\frac{Re(1-Fr^2)}{2}} e^{-z/\delta_\nu} + o\left(\nu^{-1/2}\right) \end{cases} \tag{3.7}$$

The bulk forcing f_w has the same expression at leading order for both the free-slip and the no-slip case. The difference relies in the boundary forcing expression f_{bl}.

In the free-slip case, the boundary forcing amplitude does not depend on the Reynolds number at leading order, only the width does. The amplitude decreases with the Froude number. This effect can be seen on figure 2 where the free-slip Reynolds stress is plotted for three different values of Reynolds and Froude numbers. These predictions are

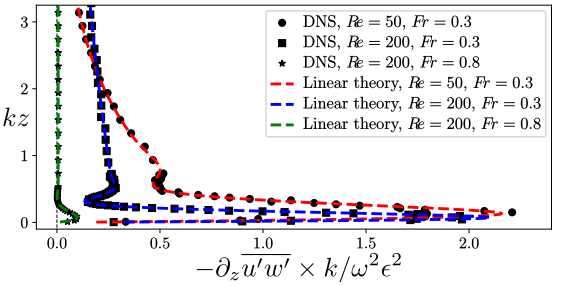

FIGURE 2. Plot of the vertical profile of the Reynolds stress in the absence of mean-flow ($\overline{u} = 0$) for the free-slip boundary condition for different couples (Re, Fr). The markers plots comes from high-resolution DNS data while the dashed lines plots comes from the linear theory. The other dimensionless parameter for the simulation are $\epsilon = 0.01$, $\tilde{\gamma} = 0$ and $R = 6kL_\nu$; the resolution is $\Delta x = \Delta z = \delta_\nu/50$; the simulated data have been smoothed over ten time steps of the simulation.

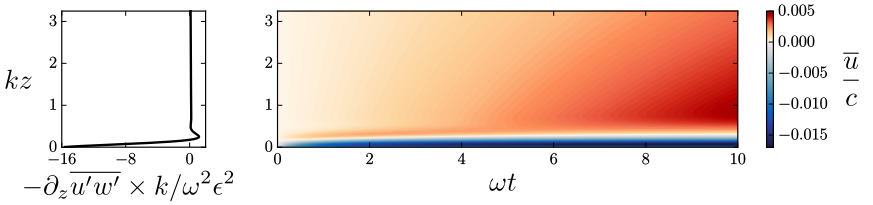

FIGURE 3. a) Plot of the vertical profile of the Reynolds stress in the absence of mean-flow ($\overline{u} = 0$) for the no-slip boundary condition computed using the linear theory, b) Hovmöller diagrams of the mean-flow predicted by the present quasi-linear model for the no-slip boundary condition. The parameters are $Re = 200$, $Fr = 0.3$, $\epsilon = 0.01$ and $\tilde{\gamma} = 0$.

successfully compared to high resolution direct numerical simulations of the established wave pattern generated by a barotropic flow above a sine-shaped topography in a linearly stratified fluid.

In the no-slip case, the Reynolds stress close to the boundary is opposite and much stronger than in the bulk, as shown in figure 3-a). According to Eq. (3.7), its amplitude scales as $Re^{1/2}$: the boundary Reynolds stress diverges in the inviscid limit. The underlying reason is the vanishing of the integral of the Reynolds stress over the whole domain.

So far we have discussed about the Reynolds stresses in the absence of mean-flows. In the next section, we compute the long time evolution of the mean-flow in the presence of those wave-induced Reynolds stresses.

4. Boundary mean-flow generation and application to an idealised model of the quasi-biennial oscillation

In order to compute the long time evolution of the mean-flow, we need to consider the presence of the mean-flow in the wave computation. We perform a WKB expansion of the wave field following the method of Muraschko *et al.* (2015) assuming that the mean-flow is sufficiently smooth. We further assume that the group velocity of the wave is infinite. The full calculation is detailed in appendix A. One can then compute the Reynolds stress and inject it into the mean-flow equation (2.4) in order to compute the long time evolution of $\overline{u}$. This task can be done numerically using the results of appendix A. We

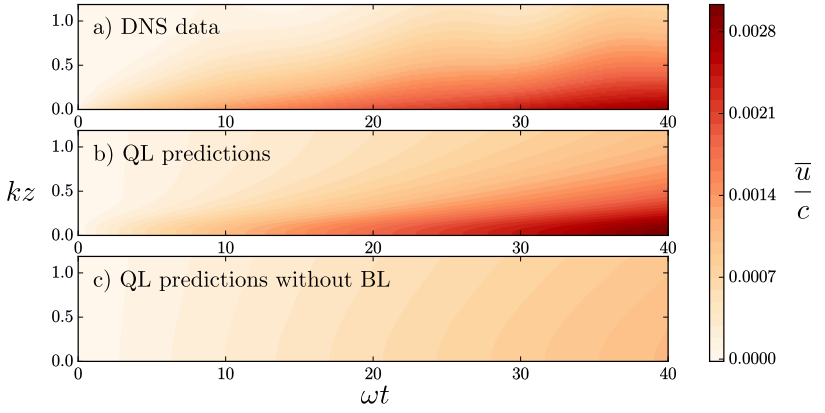

FIGURE 4. Hovmöller diagrams of the mean-flow, $\overline{u}(z,t)$. The top diagram uses the data coming from a direct numerical simulation while the diagram in the middle has been computed using the present quasi-linear model with the WKB approximation. The bottom diagram has computed using the quasi-linear model but without the boundary layer term in the wave. The parameters are $Re = 200$, $Fr = 0.3$ and $\epsilon = 0.01$. The additional numerical parameters are $\tilde{\gamma} = 0$, $R = 2kL_\nu$, $\mathrm{d}x = \mathrm{d}z = \delta_\nu/15$.

performed the computation for both the free-slip and the no-slip boundary conditions in (2.6).

On figure 4, we compare the quasi-linear predictions for the free-slip boundary condition against a direct numerical simulation. The parameters are $Re = 200$, $Fr = 0.3$ and $\epsilon = 0.01$. For those parameters, the wave boundary layer thickness is $k\delta_\nu = 0.1$ and the viscous damping length is $kL_\nu = 5.15$.The Hovmöller diagrams focus on an area close to the bottom boundary. The DNS uses a vertical resolution of $k\mathrm{d}z = 0.025$ which resolves properly the wave boundary layer length scale. We used a stretched grid on the vertical to act as a sponge layer to avoid any downward reflection. The quasi-linear model captures well the boundary streaming effect. To emphasize the crucial role of the boundary streaming term, we added a diagram on figure 4 of a quasi-linear computation where we removed the boundary layers terms in the wave expression ($f_{bl}(z) = 0$ in (3.6)). We clearly see that the effect of the boundary streaming is important to predict well the mean-flow evolution in this case.

In figure 3 b), we show a Hovmöller diagram of the mean-flow computed using the present quasi-linear model in the case of no-slip boundary condition. The parameters are, $Re = 200$, $Fr = 0.3$ and $\epsilon = 0.05$. As expected from previous discussions below (3.7), the boundary forcing generates a strong boundary mean-flow going in the opposite direction of the bulk mean-flow. Interestingly, the boundary flow saturates quickly and acts as a modified boundary condition for the bulk flow.

To illustrate how boundary streaming can affect mean-flow properties in the bulk, we apply the present quasi-linear computation to the case of a standing wave pattern for the bottom boundary, with $h(x,t) = h_b \cos(kx)\cos(\omega t)$ and no-slip conditions. Two counter propagative linear waves with equal amplitude are emitted by such a bottom excitation. Their zonal phase velocities are respectively $c = \omega/k$ and $-c$. The Reynolds stress associated with the combination of those two viscous waves is simply the sum of the Reynolds stresses associated with each wave individually. This configuration has been studied experimentally by Plumb & McEwan (1978). They reported the spontaneous generation of an oscillating zonal flow when the wave amplitude exceed a threshold, and noticed strong similarities with the quasi-biennial oscillations of low latitude stratospheric

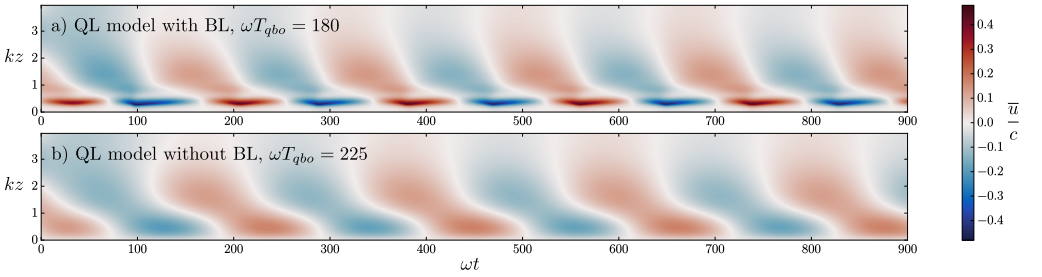

FIGURE 5. Hovmöller diagram of the mean-flow generated by the streaming coming from two equal but counter propagative waves generated by a vertically oscillating bottom boundary with no-slip condition. The parameters are $Re = 10$, $Fr = 0.2$, $\tilde{\gamma} = 0.15$ and $\epsilon = 0.1$. The period of the oscillations is $\omega T_o = 180$ with the boundary streaming and $\omega T_o = 225$ without.

winds. Plumb & McEwan (1978) compared their measurements against a quasi-linear computation neglecting the presence of a boundary layer for the waves. We plot a Hovmöller diagram of the mean-flow oscillations computed using the quasi-linear model with and without the contribution from the boundary layer terms on figure 5 a) and b) respectively. We see that in the presence of the wave boundary layer, the mean-flow oscillations are four times bigger in amplitude close to the bottom boundary, and the period of the oscillations are 20% smaller. The increase of bottom velocities due to boundary streaming favours the emergence of critical layers ($\overline{u} = \pm c$) close to the boundary. The quasi-linear model breaks down in the presence of such critical layers, where the vertical group velocity vanishes. It suggests that the presence of the linear boundary layer can lead to non-linear behaviour through boundary streaming only.

5. Conclusion

We have shown that changing the boundary conditions has a drastic impact on the boundary mean-flow generated by internal waves emitted from an undulating wall in a viscous stratified fluid. In particular, Reynolds stresses close to the boundary diverge with the Reynolds number in the case of no-slip boundary conditions, while their remain bounded in the free-slip case. Using a novel WKB treatment of the waves that takes into account viscous effects, we have also shown that boundary streaming has a substantial impact on the flow in the bulk, as we observed a 20% drop for the period of the large scale flow reversals in the idealised model of the quasi-biennial oscillation by Plumb & McEwan (1978) when taking into account boundary streaming. The control of bulk properties by boundary layers shows the importance of describing properly the physical processes taking place at these boundaries to properly predict large scale flow reversals.

We have neglected the diffusion in the buoyancy equation which involves additional diffusive boundary layers that could modify the boundary streaming. By restricting ourselves to a quasi-linear approach, we have also neglected nonlinear effects that may become important close to the boundary even in the limit of weak undulations, due to the emergence of the strong boundary current. These effects could deserve a particular attention is future numerical and laboratory experiments.

The authors warmly thank Louis-Philippe Nadeau for his help with the MIT-GCM, and express their gratitude to Freddy Bouchet and Thierry Dauxois for useful insights.

Appendix A. WKB expansion of viscous internal gravity wave within a weakly sheared mean-flow frozen in time

We compute here the leading order terms of a Wentzel-Kramers-Brillouin (WKB) expansion of the viscous wave field within a weakly sheared mean-flow frozen in time. We follow the method developed in Muraschko *et al.* (2015), the novelty being the presence of viscosity, in the wave equation (2.5). We assume that the mean-flow, $\overline{u}$, defined in (2.3), is frozen in time and depends only on the smooth variable $Z = az$ with $a \ll 1$. We introduce a WKB ansatz:

$$\begin{bmatrix} u' \\ w' \\ b'/N \\ p' \end{bmatrix} = \Re\left\{ \sum_{j=0}^{+\infty} a^j \begin{bmatrix} \tilde{u}_j(Z) \\ \tilde{w}_j(Z) \\ \tilde{b}_j(Z)/N \\ \tilde{p}_j(Z) \end{bmatrix} \exp\left\{ ik(x-ct) + \frac{i\Phi(Z)}{a} \right\} \right\} \tag{A 1}$$

where c is the phase speed of the wave. The function $\Phi(Z)$ accounts for the vertical phase progression of the wave. The local vertical wave number is defined by $m(Z) = \partial_Z \Phi$. Injecting this expansion into the previous equation and collecting the leading order terms in a leads to:

$$\boldsymbol{M} \begin{bmatrix} \tilde{u}_0 \\ \tilde{w}_0 \\ \tilde{b}_0/N \\ \tilde{p}_0 \end{bmatrix} + a \left(\boldsymbol{M} \begin{bmatrix} \tilde{u}_1 \\ \tilde{w}_1 \\ \tilde{b}_1/N \\ \tilde{p}_1 \end{bmatrix} + \begin{bmatrix} \tilde{w}_0 \partial_Z \overline{u} - i\nu\left(\tilde{u}_0 \partial_Z m + 2m\partial_Z \tilde{u}_0\right) \\ \partial_Z \tilde{p}_0 - i\nu\left(\tilde{w}_0 \partial_Z m + 2m\partial_Z \tilde{w}_0\right) \\ 0 \\ \partial_Z \tilde{w}_0 \end{bmatrix} \right) + o(a) = 0 \tag{A 2}$$

with

$$\boldsymbol{M} = \begin{bmatrix} -ik(c-\overline{u})\left(1 + \frac{\nu\left(k^2+m^2\right)+\gamma}{k(c-\overline{u})}\right) & 0 & 0 & ik \\ 0 & -ik(c-\overline{u})\left(1 + \frac{\nu\left(k^2+m^2\right)+\gamma}{k(c-\overline{u})}\right) & -N & im \\ 0 & N & -ik(c-\overline{u}) & 0 \\ ik & im & 0 & 0 \end{bmatrix}. \tag{A 3}$$

We introduce the polarization $\mathbf{P}[m]$ defined by $\left[\tilde{u}_0, \tilde{w}_0, \tilde{b}_0/N, \tilde{p}_0\right] = \phi_0(Z)\,\mathbf{P}[m]$, where $\phi_0(Z)$ is the dimensionless amplitude of the wave mode. The cancellation of the zeroth order term in Eq. (A 1) yields to $\det \boldsymbol{M} = 0$. This gives the local dispersion relation

$$(c-\overline{u})^2 \left(1 + i\frac{\nu\left(k^2+m^2\right)+\gamma}{k(c-\overline{u})}\right) = \frac{N^2}{k^2+m2}. \tag{A 4}$$

Then, using $\boldsymbol{M} \cdot \mathbf{P} = 0$ we obtain the polarization expression

$$\mathbf{P}[m] = \left[c-\overline{u}, -\frac{k}{m}(c-\overline{u}), \frac{iN^2}{m}, \frac{N^2}{k^2+m2}\right]. \tag{A 5}$$

The cancellation of the terms proportional to a in (A 2) provides an equation for the amplitude $\phi_0(Z)$. To get rid of the terms involving components of the order one wave, we look for a vector $\mathbf{P}^*$ such that $\mathbf{P}^* \cdot \boldsymbol{M} = \mathbf{0}$. We then take the inner product between $\phi_0 \mathbf{P}^*$ and the terms proportional to a in (A 2). Introducing $\varphi_0^2 = \phi_0^2 (c-\overline{u})^2 / m$, we obtain after long but straightforward algebra :

$$\partial_Z \log \varphi_0^2 + \frac{2i\nu}{k(c-\overline{u})} \partial_Z m^2 = 0 \tag{A 6}$$

This last equation has to be solved for every solution $m(Z)$ of the dispersion relation. In the limit $\nu \to 0$, we recover the inviscid result obtained by Muraschko *et al.* (2015).

REFERENCES

Adcroft, A., Hill, C. & Marshall, J. 1997 Representation of topography by shaved cells in a height coordinate ocean model. *Monthly Weather Review* **125** (9), 2293–2315.

Baldwin, M.P., Gray, L.J., Dunkerton, T.J., Hamilton, K., Haynes, P.H., Randel, W.J., Holton, J.R., Alexander, M.J., Hirota, I., Horinouchi, T., Jones, D.B.A, Kinnersley, J.S., Marquardt, C., Sato, K. & Takahashi, M. 2001 The quasi-biennial oscillation. *Reviews of Geophysics* **39** (2), 179–229.

Beckebanze, F. & Maas, L. 2016 Damping of 3d internal wave attractors by lateral walls. *Proceedings, International Symposium on Stratified Flows* .

Bordes, G., Venaille, A., Joubaud, S., Odier, P. & Dauxois, T. 2012 Experimental observation of a strong mean flow induced by internal gravity waves. *Physics of Fluids* **24** (8), 086602.

Bühler, O. 2009 *Waves and Mean Flows*. Cambridge University Press.

Gostiaux, L., Didelle, H., Mercier, S. & Dauxois, T. 2006 A novel internal waves generator. *Experiments in Fluids* **42**, 123–130.

Grisouard, N. & Bühler, O. 2012 Forcing of oceanic mean flows by dissipating internal tides. *Journal of Fluid Mechanics* **708**, 250–278.

Kataoka, T. & Akylas, T.R 2015 On three-dimensional internal gravity wave beams and induced large-scale mean flows. *Journal of Fluid Mechanics* **769**, 621634.

King, B., Zhang, H. P. & H. L. Swinney, Harry L 2009 Tidal flow over three-dimensional topography in a stratified fluid. *Physics of Fluids* **21** (11), 116601.

Legg, S. 2014 Scattering of low-mode internal waves at finite isolated topography. *Journal of Physical Oceanography* **44** (1), 359–383.

Lighthill, J. 1978 Acoustic streaming. *Journal of Sound and Vibration* **61** (3), 391 – 418.

Maas, L., Benielli, D., Sommeria, J. & Lam, F. A. 1997 Observation of an internal wave attractor in a confined, stably stratified fluid. *Nature* **388** (6642), 557–561.

Muraschko, J., Fruman, M. D., Achatz, U., Hickel, S. & Toledo, Y. 2015 On the application of wentzel-kramer-brillouin theory for the simulation of the weakly nonlinear dynamics of gravity waves. *Quarterly Journal of the Royal Meteorological Society* **141** (688), 676–697.

Nikurashin, M. & Ferrari, R. 2010 Radiation and dissipation of internal waves generated by geostrophic motions impinging on small-scale topography: Application to the southern ocean. *Journal of Physical Oceanography* **40** (9), 2025–2042.

Plumb, R. A. & McEwan, A. D. 1978 The instability of a forced standing wave in a viscous stratified fluid: A laboratory analogue of .the quasi-biennial oscillation. *Journal of the Atmospheric Sciences* **35** (10), 1827–1839.

Riley, N. 2001 Steady streaming. *Annual Review of Fluid Mechanics* **33** (1), 43–65.

Semin, B., Facchini, G., Pétrélis, F. & Fauve, S. 2016 Generation of a mean flow by an internal wave. *Physics of Fluids* **28** (9), 096601.

Shakespeare, C. J. & Hogg, A. McC. 2017 The viscous lee wave problem and its implications for ocean modelling. *Ocean Modelling* **113**, 22 – 29.

Sutherland, B. R. 2010 *Internal gravity waves*. Cambridge University Press.

Voisin, B. 2003 Limit states of internal wave beams. *Journal of Fluid Mechanics* **496**, 243293.

Xie, J. & Vanneste, J. 2014 Boundary streaming with navier boundary condition. *Physical Review E* **89** (6).

Zarembo, L. K. 1971 *High-Intensity Ultrasonic Fields*, chap. Acoustic streaming, p. 156174. New York: Plenum.